Genetic architecture of pollination syndrome transition between hummingbird-specialist and generalist species in the genus *Rhytidophyllum* (Gesneriaceae)

Hermine Alexandre, Justine Vrignaud, Brigitte Mangin, Simon Joly

Adaptation to pollinators is a key factor of diversification in angiosperms. The Caribbean sister genera *Rhytidophyllum* and *Gesneria* present an important diversification of floral characters. Most of their species can be divided in two major pollination syndromes. Large-open flowers with pale colours and great amount of nectar represent the generalist syndrome, while the hummingbird-specialist syndrome corresponds to red tubular flowers with a less important nectar volume. Repeated convergent evolution toward the generalist syndrome in this group suggests that such transitions rely on few genes of moderate to large effect. To test this hypothesis, we built a linkage map and performed a QTL detection for divergent pollination syndrome traits by crossing one specimen of the generalist species *Rhytidophyllum auriculatum* with one specimen of the hummingbird pollinated *R. rupincola*. Using geometric morphometrics and univariate traits measurements, we found that floral shape among the second-generation hybrids is correlated with morphological variation observed between generalist and hummingbird-specialist species at the genus level. The QTL analysis showed that colour and nectar volume variation between syndromes involve each one major QTL while floral shape has a more complex genetic basis and rely on few genes of moderate effect. Finally we did not detect any genetic linkage between the QTLs underlying those traits. This genetic independence of traits could have facilitated evolution toward optimal syndromes.

HERMINE ALEXANDRE*1, JUSTINE VRIGNAUD*, BRIGITTE MANGIN[§,†], SIMON JOLY*

* Institut de Recherche en Biologie Végétale, Université de Montréal, 4101 Sherbrooke East, Montreal QC H1X2B2, Canada

[§] INRA, Laboratoire des Interactions Plantes-Microorganismes (LIPM), UMR441, F-31326 Castanet-Tolosan, France

[†] CNRS, Laboratoire des Interactions Plantes-Microorganismes (LIPM), UMR2594, F-31326 Castanet-Tolosan, France

1 : corresponding author :

Hermine Alexandre

hermine.alexandre@umontreal.ca

Institut de Recherche en Biologie Végétale, Université de Montréal, 4101 Sherbrooke East, Montreal QC H1X2B2, Canada

514-343-6111 ext. 82121

INTRODUCTION

Adaptation corresponds to "the movement of a population towards a phenotype that best fits the present environment" (Orr, 2005). The ability of species to adapt to their environments is one of the main factors of evolutionary success. In angiosperms, which rely on pollination to reproduce, adaptation of the pollination system to the available environment - that is available pollinators - is a key for achieving successful reproduction and maintaining optimal fitness.

It is often possible to distinguish patterns in groups of traits that evolve jointly for the flower to be effectively pollinated by a given type of pollinator. These groups of traits are called pollination syndromes (Fenster et al., 2004). The selection for these syndromes is often so strong that it is possible to predict on which type of pollinator a given plant species rely. For instance, flowers can harbour very different traits depending on whether they are pollinated by wind or animals (Friedman & Barrett, 2009); for example *Plantago* presents a wind-pollination syndrome characterised by small radially symmetrical flowers (Preston, Martinez & Hileman, 2011). In animal-pollinated groups, major traits involved in pollination syndrome include corolla shape and colour, floral scent, as well as the amount and concentration of nectar produced, and variation at these traits enable to distinguish species pollinated by different functional groups of animals. Rosas-Guerrero et al. (2014) reviewed floral traits of 417 species and showed that the concept of pollination syndrome is very effective at predicting the syndrome of animal pollinated flowers, more so than for non-animal syndromes. Interestingly, this concept is more efficient for tropical plants, probably because of lower pollinator population densities in the tropics that increase selection pressure (Rosas-Guerrero et al., 2014).

Pollination syndrome is a set of very dynamic and rapidly evolving characters and offers classic examples of convergent evolution in many groups. In *Penstemon* (Plantaginaceae), for example, ornithophilous pollination evolved multiple times from insect pollinated flowers (Wilson et al., 2007). In *Ruellia*, insect pollination evolved repeatedly from the ancestral hummingbird pollination (Tripp & Manos, 2008). In *Gesneria* and *Rhytidophyllum* (Gesneriaceae), generalist and bat pollinated species evolved several times from a hummingbird syndrome (Martén-Rodríguez et al., 2010). The tribe Sinningieae of the Gesneriaceae also shows an important lability of pollination-associated traits such as corolla shape and colour (Perret et al., 2007). Because such transitions between syndromes are often linked with species diversification (reviewed in van der Niet and Johnson 2012), understanding how these transitions occur is critical for understanding angiosperms evolution.

Observations of such an important lability of flower characters, combined with the fact that it is a motor of species diversification, raise the question of how these traits are genetically determined. Some of the main questions in studies of the genetic bases of phenotypic evolution are (i) do parallel phenotypic changes rely on parallel genotypic evolution and (ii) do these major phenotypic transitions result from few genes with major effect or do they rely on multiple minor genetic changes (reviewed in Hendry 2013). In addition, developmental constraints such as genetic interactions (epistasy) could be important to explain the convergence of different traits to form a particular syndrome. Similarly, we might want to investigate the respective roles of genetic correlations between traits and ecological factors – such as pollinator pressures – in the redundant evolution of floral phenotypes among different species. Indeed, the speed at which a population reaches its fitness optimum greatly depends on whether traits composing the pollination syndrome are genetically independent or linked. We can envision three scenarios: (i) if traits are positively correlated, selection on one trait will affect variation at other traits in a positive way and the general fitness optimum should be reached rapidly; (ii) if traits are genetically independent, no developmental constraints should affect the evolution towards the optimum; and (iii) if traits are negatively correlated, selection at one trait will pull variation at other traits further form the fitness optimum, hence reducing the pace at which this optimum can be reached. Deciphering the degree of genetic correlation among traits is thus a first step toward understanding the relative role of selection versus intrinsic constraints in the evolution of phenotypes (Ashman & Majetic, 2006).

To answer these questions, a popular approach is to perform QTLs detection on a hybrid population issued from parents with different pollination syndromes. Previous studies have shown that colour transition is generally explained by one major QTL (Quattrocchio et al. 1998; Yuan et al. 2013; Wessinger et al. 2014). In contrast, nectar volume and concentration frequently rely on numerous genomic regions each having a small to moderate effect on phenotype (Goodwillie, Ritland & Ritland, 2006; Galliot et al., 2006; Nakazato, Rieseberg & Wood, 2013). Flower shape variation was also shown to be generally caused by several QTLs with small to moderate effects, with frequent colocalization of those QTLs (reviewed in Hermann and Kuhlemeier 2011). During the past several years, emerging new generation sequencing technologies have enabled and facilitated the study of the genetic bases of adaptation in non-model species. As well, improvements of methods to study morphology, principally with geometric morphometrics, now enable to study the genetic bases and

evolution of these complex characters (Klingenberg et al. 2001; Langlade et al. 2005; Klingenberg 2010; Rogers et al. 2012; Franchini et al. 2014; Liu et al. 2014).

The closely related genera *Gesneria* and *Rhytidophyllum* that consist of approximately 60 species have rapidly diversified in the Antilles from a common ancestor that existed approximately 8 to 11 mya (Roalson et al. 2008). Simultaneously to this rapid species diversification, the group also experienced a rapid diversification of floral traits. Floral shape, colour and nectar production have evolved jointly into three evolutionarily labile pollination syndromes (Martén-Rodríguez, Almarales-Castro & Fenster, 2009, Martén-Rodríguez et al. 2010): (i) species pollinated by hummingbirds have tubular and red flowers with diurnal nectar production, (ii) species pollinated by bats harbour large pale flowers with a bell shape corolla and with nocturnal nectar production, and (iii) generalist species that can either be pollinated by hummingbirds, bats or moths, have pale flowers (although often with various spots) with large openings but with a constriction in the corolla, and can have nocturnal and diurnal nectar production. The hummingbird syndrome was inferred as the ancestral pollination mode and generalist and bat syndromes evolved several time independently, with some reversals to the ancestral hummingbird pollination (Martén-Rodríguez et al., 2010). We intend here to identify the genetic bases of pollination syndrome transition between generalist and bird-specialist species in *Rhytidophyllum* using QTL detection in a second-generation hybrid population. *Rhytidophyllum auriculatum* is a typical generalist species originating from Hispaniola, and harbours opened yellow flowers producing large amount of nectar. The second species, *R. rupincola*, is a hummingbird specialist with red and tubular flowers that produces only small quantities of nectar. Its endemism to Cuba (Skog 1976; Martén-Rodríguez et al. 2010; pers. Obs.) eliminates all potential for natural hybridization with *R. auriculatum*. According to Marten Rodriguez et al. (2010), *R. auriculatum* belong to a group of generalist that evolved from an ancestral hummingbird syndrome, whereas *R. rupincola* likely represents a reversion to the ancestral hummingbird syndrome. The two species are closely related but are not sister species (Marten Rodriguez et al. 2010).

In this study, we obtained anonymous genetic markers via next generation sequencing (NGS) and built a linkage map from a second generation (F2) hybrid population between *R. rupincola* and *R. auriculatum*. We then used geometric morphometrics to study floral shape and test whether QTLs underlying floral trait evolution are few or numerous and whether they are linked or not.

MATERIAL AND METHODS

Study system:

Rhytidophyllum auriculatum (female parent) was crossed with *R. rupincola* (male parent) from specimens from the living collection of the Montreal Botanical Garden (Canada) in 2010 to obtain first-generation (F1) hybrids. One F1 individual was self-fertilized in 2011 to give a second-generation (F2) population of 177 individuals. In parallel, both parents were self-crossed and gave several viable individuals.

Phenotypic measurements:

Phenotypic measures were performed from June of 2013 to April 2014 for morphological and colour traits because of a great heterogeneity of developmental rate in the population. Color was binary coded as either yellow or orange; the latter category included all corollas that contained some orange. Corolla shape was analysed with geometric morphometrics methods to capture morphological components that are characteristic of pollination syndromes without a priori hypotheses. In addition to allow determining the shape representative of a particular pollination mode, geometric morphometric methods were shown to be very efficient to study the genetic bases of morphological changes (Klingenberg et al. 2001).

For each individual we photographed between one and three flowers. Each photo was analysed twice with the software TpsDIG2 (http://life.bio.sunysb.edu/morph/soft-dataacq.html), to evaluate variance due to manipulation errors in our analyses. We also included photographs from a different study (Joly et al. in prep) that aimed at quantifying shape variation in the whole *Gesneria/Rhytidophyllum* clade in order to characterize the aspects of shape that were the most significant to differentiate generalists from hummingbird specialists (see below). For these photograph, a single flower per individual was included. We placed 6 landmarks and 24 semi-landmarks on each photo. Two landmarks were placed at the extremity of the petal lobe (L1, L2), two at the base of the petal lobes (L3, L4) and two at the base of the corolla (L5, L6). Semi-landmarks were evenly dispersed on the contour of the corolla between L3-L4 and L5-L6 (Fig. 1). Geometric morphometrics analyses were then performed in R (R Development Core Team 2008) with packages shapes (Dryden, 2014), geomorph (Adams & Otárola-Castillo, 2013) and ade4 (Dray & Dufour, 2007). We performed a general Procrustes superimposition

of all the photos with the function *gpagen* allowing for sliding semi-landmarks in the superimposition, and extracted the mean coordinates of the landmarks and semi-landmarks per individual to get only one shape per individual. Morphology was then measured using four approaches to address the problem from different facets (see Fig. 2 for more details): (i) a PCA (function *dudi.pca*) was done on nine generalist and nine hummingbird specialist species data from the genera (see supplementary Table 1 for details) and the F2 individuals were projected onto this PCA (function *suprow*); (ii) a PCA was performed on the two parents and the F2 individuals were projected on this PCA; (iii) a PCA was performed directly on the F2 population (including the selfed F1, both parents and three parents' progenies) – hereafter referred as PCA on the hybrid population; (iv) we extracted two univariate traits from the landmarks data before Procrustes superimposition: corolla tube opening corresponds to the distance between L3 and L4 and corolla curvature is the angle formed by the lines (L1-L2) and (L5-L6) (Fig. 1). Pictures from wild specimens were uniquely used to analyse shape, without any size component because photos did not include a scale. Four F2 individuals with abnormal flowers (disjoint petals or different flower shapes within an individual) were discarded from the phenotypic measures.

Measurements of nectar volume were done between November and December 2014. Nectar was sampled in early afternoon after anthesis, which generally occurs two days after flower opening. This time was chosen because nectar is released mainly at dawn and dusk in *Gesneria* and *Rhytidophyllum* (Martén-Rodríguez & Fenster, 2008), and because we observed no nectar production during the day for the parental species. To sample nectar, the flowers were removed from the plant, and the volume was measured with a graduated 50 µL syringe.

Genotyping:

Leaves from young plants were sampled and dried in silica gel, and DNA was extracted with the Qiagen (Mississauga, Canada) DNeasy Plant Mini Kit. 300 ng of DNA were used to genotype individuals using a Genotyping By Sequencing approach, following the protocol developed by Elshire et al. (2011). Library preparation was performed at Laval University (IBIS plateform, Quebec city, Canada) using the restriction enzymes *Pst*I and *Msp*I. We sequenced 177 F2s, duplicating ten individuals to assess genotyping repeatability: four F2s, both parents, the self-crossed F1 and three other F1s, and two progenies of the selfed parents. Individuals were multiplexed, and sequenced on two Illumina Hiseq 2500 lanes at McGill University and Génome Québec Innovation Centre (Montreal, Canada). Stacks pipeline version 1.20 Beta was used to extract genotypes from raw reads

(Catchen et al., 2011). Reads were first demultiplexed and trimmed to 82 basepairs with the function process-radtags. Then, we generated unique stacks with the function ustacks, constraining for a minimum read depth (-m) of 2 to create a stack, and a maximum inter-read Single Nucleotide Polymorphism (SNP) distance (-M) of 5. The catalog was created with both parents, and SNP calls were first performed with default parameters in sstacks. We then ran the error correction module rxstacks to perform automated corrections using the bounded SNP model and a cutoff ln likelihood value of -10 to discard unlikely genotypes. Then we ran again cstacks and sstacks with the corrected data, and genotypes data were obtained with the function genotypes. After running genotypes with the –GEN output format and allowing automatic corrections with default parameters, we ran a home-made R script to translate those data in a A (parent *R. auriculatum* allele), B (parent *R. rupincola* allele), H (heterozygous) format needed for subsequent analyses. In this script, using the information available from the selfed F1, we allowed markers that are aaxab in the parents, and for which the F1 is ab to be typed in the F2 population. This step was necessary because the Stacks pipeline would not have recognized these as valid markers.

We used the same DNA extractions to genotype two candidate genes: *CYCLOIDEA* and *RADIALIS*, known to be involved in flower morphology development (Preston, Martinez & Hileman, 2011). Genes sequences acquired from GenBank (sequence AY363927.1 from *R. auriculatum* for *Gcyc* and sequence AY954971.1 from *Antirrhinum majus* for *RADIALIS*) were compared to the parents' transcriptomes (unpublished data) using BLASTn (Camacho et al., 2009) and primers were designed using software Primer3 (Koressaar & Remm, 2007). *CYCLOIDEA* was genotyped with the CAPS method (Konieczny & Ausubel 1993). Around 1 ng of DNA was added to a master mix containing 0,375 U of DreamTaq (Termoscientific, Waltham, MA, USA), 1.5 µL of 10X DreamTaq Buffer, 0.6 µL of each 10 µM primer and 0.3 µL of 10 mM dNTPs in a total reaction volume of 15 µL. Primers used to amplify *CYCLOIDEA* were gcycf2 (AAGGAGCTGGTGCAGGCTAAGA) and gcycr2 (GGGAGATTGCAGTTCAAATCCCTTGA), amplification conditions were 2 min at 94°C, followed by 40 cycles of 94°C 15 sec, 54°C 15 sec, 72°C 30 sec, and then a final extension step of 1 min at 72°C. Circa one µg of PCR products were then digested with *Afl*II (New England Biolabs, Ipswich, MA, USA) in a 15 µL volume according to the company's recommendations. The total volume of digestion products was visualized on agarose gel. *RADIALIS* was genotyped with KASPAR (LGC genomics, Teddington, UK), with protocol tuning done by LGC genomics. DNA amplification was

done with 75 ng of DNA, 2.5 µL of KASP master mix, and 0.07 µL of KASP primer mix in a total volume of 5 µL. The specific primer for the first parental allele was labelled with a FAM fluorochrome while the second specific primer was labelled with a HEX fluorochrome. Amplification conditions were a first step of 94°C for 15 min, followed by 10 cycles of 94°C 20 sec, 61°C decreasing of 0.6°C at each cycle 1 min, and then another 29 cycles of 94°C 20 sec 55°C 1 min. Genotypes were visualized by fluorescence after the amplification procedure on viia7 system (Applied Biosystems, Foster city, CA, USA) with the "genotyping" protocol.

Linkage map construction:

GBS markers were filtered to keep only those with less than 25% missing data, and no segregation distortion (χ^2 p-value > 0.05 after Bonferonni correction). A linkage map was built with Carthagene (de Givry et al., 2005). Linkage groups were detected with a maximum two points distance of 30 cM measured with Haldane function and a minimum LOD of 3. Marker ordering in each linkage group was done with the function *lkhd*, which implement the Lin-Kerninghan heuristic research algorithm to resolve the travelling salesman problem, optimising the 2 points distances along the linkage group. Once the first map was obtained, we checked for double-recombinants occurring within 10 cM and made manual corrections. Because SNP calls can be erroneous if read depth is small, we replaced double recombinants scored as either A or B (homozygous) into H (heterozygous), if read depth was less than 10 reads. If read depth was more than 10, double recombinant genotype were replaced by missing data as proposed by Kakioka et al. (2013), because those genotypes have a great probability of being erroneously typed. For H (heterozygous) double recombinants, we did not replace it if both alleles were effectively detected in the sequencing data, and we replaced it into A or B if only one allele was detected in the data (this case occurred because of wrongly corrected calls with automatic correction in stacks). Remaining markers were then filtered again for missing data and segregation distortion, and a new map was built. This was repeated until no double-recombinants within 10cM were found in the linkage map. After these cleaning steps, genotypes of both candidate genes were included in the dataset, and a final linkage map was built.

QTLs detection:

Before performing QTL detection, we tested for significant correlation between colour, nectar volume and shape traits in the F2 population using pearson coefficient for quantitative traits correlation and F-

test for tests involving colour. 141 individuals were kept for colour tests and 129 for shape QTLs detection after inappropriate data was removed. Nectar volume was transformed into a binary trait for QTL detection given its large intra-individual variation and non-normal distribution in the F2 population. Individuals with mean volume inferior to 15 µL were classified as "0" and those with a mean volume superior to 25 µL as "1", leaving 67 individuals to detect QTLs for nectar volume. QTL detection was performed with R/qtl (Broman et al., 2003). We calculated genotypes probabilities every 1cM with the function *calc.genoprob*. We looked for QTL with *scaneone* with the normal model and the Haley-Knott method for the quantitative traits; we used the binary model and the EM method for nectar volume and colour. LOD scores were compared to the LOD threshold value obtained with 10,000 permutations. Then, if a QTL was detected, it was added as an additive covariate, and *scaneone* as well as the permutations were rerun to detect minor QTLs. For non-binary variables, percentage of variance explained by the QTLs and size effects were checked with *fitqtl*, adding in the model one QTL at a time. QTL effect sizes were also measured with *fitqtl*. Given the limited number of individuals scored for nectar volume, we performed a supplementary Spearman correlation test between nectar volume (codes 0/1) and genotypic data for each marker (codes 1/2/3) to confirm the QTL results.

Pleiotropy and epistasy detection:

Pleiotropic QTLs were searched by considering the principal axes of the PCA done on the hybrid population as proposed by Mangin et al. (1998). We limited the computation of the pleiotropic test statistics by considering only the first three principal axes, which explained most of the variance, as suggested by Weller et al. (1996). Briefly, the test was obtained by computing the LOD scores for each principal component, and summed the result over all the three principal components. To access the threshold value of the pleiotropic test statistics, we performed 10,000 permutations (Doerge & Churchill, 1996) with the three principal components being permutated all together in order to get a null distribution, while preserving the initial correlation between the phenotypic traits. QTL detection was based on the 95th quantile. Confidence regions were estimated with a 2-LOD support, as suggested by Van Ooijen (1992). Epistasy among QTLs as well as among QTLs and other markers were tested using MCQTL (Jourjon et al., 2005).

Scripts and data used for morphometric analyses, map building and QTLs detection are available as supplementary data.

RESULTS

Correlation between traits and morphological variation:

On the PCA done on the 18 species with divergent pollination syndromes (approach i), the first principal component (PC1: 68.55%) discriminated hummingbird specialist species from generalists (Fig. 3a). Interestingly, both parents were positioned within their respective pollination syndrome group and the selfed F1 and the F2 population were intermediate between both syndromes on the first principal component. As only the first principal component separated the two syndromes, only this component was used for QTL detection. The Principal component analysis performed on the hybrid population (approach iii) explained the majority of morphological variability found in the hybrid population (PC1: 35%, PC2: 22.7%, PC3: 14.2%, total=71.9%; Fig. 3b). On this PCA, parents were at the extremities of the distribution, the selfed F1 was intermediate between parents and the F2s represented a cloud of points between parents. Interestingly, the F2 individuals were closer to *R. rupincola* than *R. auriculatum* (Fig. 3b).

On the genus level, PCA done on species the 18 harbouring divergent pollination syndromes, the first principal component discriminate hummingbird specialist species from generalist ones. Interestingly, both parents localized with their respective pollination syndrome group and the selfed F1 and the F2 population were intermediate between both syndromes on the first principal component (Fig. 3 a). As only the first principal component can separate the two syndromes, only this component was used for QTL detection. Morphological variation associated with each principal component can be visualized on Fig. 4. We measured correlation between morphological principal components and two univariate traits (constriction size, the corolla curvature) as well as two binary traits (corolla colour, nectar volume). Traits corresponding to different pollination syndrome components (shape, colour, nectar) were not correlated among individuals of the F2 population (Fig. 5), which suggest that those components are genetically independent. However, the first principal component of each PCA (performed on the genus, both parents or the hybrid population) are correlated with each other with high correlation coefficient (first PC on the genus – first PC on the hybrid population: r=0.98; first PC on the genus – PC on the

parents: r=0.901; first PC on the hybrid population – PC on the parents: r=0.811, Fig. 5). As well, principal components of PCA are correlated with univariate shape measures (second PC on the hybrid population-corolla curvature: r=-0.92; constriction size-first PC on the genus: r=-0.633, Fig. 5).

Molecular data and linkage map:

Starting from ca. 422 millions raw reads, the stacks pipeline gave 2,257 markers. After removing markers with more than 25% missing data and with segregation distortion, 845 markers remained to construct a genetic map. Then, with the third step of iterative map building, following correction for double recombinants and filtering for missing data, we finally obtained 557 clean GBS and two candidate-genes markers. With a maximum distance of 30cM (between consecutive markers) and a minimum LOD score of 3, 16 linkage groups were identified. Groups remained stable even if the LOD threshold was changed from 1 to 10, which is suggestive of a relatively good stability of our linkage groups. The linkage map represents a total length of 1650.6 cM with an average distance between adjacent markers of 3.39 cM and relatively heterogeneous linkage group size (Table 1 and Fig. 6). Recombination fractions and 2-points LOD scores can be visualised of supplementary Fig. 2.

QTLs analysis:

QTLs for simple traits

Flower colour was treated as a binary trait: orange or yellow. Given the large variation in intensity and distribution of the orange colour on the corolla (Fig. 1), individuals were considered “orange” when some orange colour was observed on them. The ratio of yellow to orange flowered individuals in the 177 genotyped F2s was of 42:99, which is not significantly different from a 1:3 ration expected for a dominant Mendelian marker (χ^2 test $\chi^2 = 1.7234$; p-value = 0.1893). A single QTL, on linkage group LG16, was found to explain colour variation in the F2 population (Fig. 6).

We detected one QTL explaining nectar volume differences on LG12, with a very large confidence region (123.4 cM). As for colour, we could not measure the amount of variance explained by this QTL because we used transformed data (binary model). These results were confirmed by correlation between the traits and markers as only two markers, both on LG12, were significantly correlated to nectar after a Bonferonni correction (position 46.1, p-value = 2.78E-06; position 56.3, p-value = 4.19E-05).

We measured shape with geometric morphometrics and with univariate measures. For the shape variation between pollination syndromes (approach i) we detected three distinct QTLs on LG1, LG11, and LG14 explaining respectively 12.8%, 13.6% and 8.8% of variance (Fig. 6; Table 2). For the shape variation between parents (approach ii) we also detected three QTLs on LG13, LG11 and LG14 explaining 6.7%, 10.2% and 12.8% of the variance (Fig. 6; Table 2). When measuring morphological variation in the F2 hybrids (approach iii), we selected three shape components. One QTL controlling the first component on LG1 and explaining 15.1% of the variance was identified, while one QTL on LG2 explaining 14% of the variance for the second component, and one QTL on LG9 explaining the 14.9% of variance for the third component were identified (Fig. 6; Table 2). Corolla tube opening variation was explained by 2 QTL on LG1 and LG16 explaining 12.5% and 12.4% of the variance, respectively. Corolla curvature was explained by one QTL on LG2 representing 12.8% of the variance.

Interestingly, the same QTLs were detected irrespective of the way morphology was quantified (Fig. 6), that is, co-localizing QTLs were detected for co-varying traits. For instance, the QTL on LG1 was detected with the different methods used to measure shape. This specific QTL on LG1 was detected using the principal component that distinguished generalists and specialists as well as using corolla tube constriction. Considering all shape analyses together, a total of seven different QTLs were detected, which explained small to moderate part of morphological variance (Table 2).

We found that one candidate gene for floral shape, *CYCLOIDEA*, co-localized with a QTL confidence region for corolla constriction, although the position of the gene does not correspond to the maximum LOD value (Fig. 6 and Table 2). *RADIALIS* did not co-localize with any QTLs.

Pleiotropic and epistatic QTLs

When analyzing QTLs acting pleiotropically on the three first shape components obtained from the PCA on the hybrid population, we detected one QTL on LG1 co-localizing with QTL for simple traits. Epistasy analysis was conducted with MCQTL and no epistatic interaction was detected among QTLs and neither among QTLs and other markers.

DISCUSSION

Detection of moderate QTLs involved in pollination syndrome transition:

Our linkage map construction was able to recover 16 linkage groups. This is two more than the haploid chromosome number (*n*=14) for *Rhytidophyllum* (Skog 1976). However, if karyotype information exists for *R. auriculatum* (Skog 1976), none exist specifically for *Rhytidophyllum rupincola*. Yet, an *n*=14 for *R. rupincola* appears likely because all *Rhytidophyllum* species studied so far are *n*=14. In addition, differences in chromosome number between the parents seem unlikely given the viability of second generation hybrids. Finding more than 14 linkage groups might result from low genome coverage. However, the hypothesis of low genome coverage that would have prevented from assembling linkage groups together seems unlikely because the average distance between consecutive markers is quite small. Yet, the parents of the cross are from distinct species and chromosomal rearrangements could have occurred between them. These could create difficulties in assigning some chromosomal segments to the rest of the chromosome; the smallest linkage groups could thus correspond to rearranged chromosomal regions between both species.

Colour differences QTL

We detected one QTL explaining colour transition between *R. auriculatum* and *R. rupincola*. While this result might be influenced by the fact that colour was coded as a binary trait, we are confident that it reflects a true aspect of colour evolution in this group. The reason why we studied colour as a binary trait is first that there is a gap between yellow and orange flowers in our population (even if there is an important variation in orange pigmentation), with proportions (1:3) concordant with the pattern of a phenotype governed by a unique Mendelian segregating gene. Secondly, most generalist species harbour pale colours while the majority of hummingbird specialists are red (Martén-Rodríguez et al., 2010). The results presented here are concordant with previous studies on pollination syndrome transitions that investigated the genetic basis of colour variation. Wessinger et al. (2014) found one QTL for colour, corresponding to a gene involved in anthocyanin biosynthesis pathway. Similarly, the famous case of colour transition in *Mimulus* showed that a single mutation at the *YUP* locus can both affect flower colour and pollinators behaviour (Bradshaw & Schemske 2003). However, we observed an important variation of colour patterns among orange flowers in the hybrid population, both in terms of intensity and localisation of pigments. This suggests that other genes could be involved in the intensity and distribution pattern of pigments, probably through differential gene expression over the corolla. Other studies on genetic bases of colour transitions suggest that colour transitions generally involve degeneracy in a gene of pigment biosynthesis pathway (Galliot, Stuurman & Kuhlemeier,

2006). Future work will then involve the study of the association between colour pattern and the expression of major genes in the anthocyanin biosynthesis pathway.

Nectar volume QTL

Similarly to colour, we detected a single QTL for nectar volume differences. We did not plan to code nectar volume as a binary trait initially, but a large intra-individual variance coupled with a non normal distribution of this trait in the population and a small sample size (because of mortality between the moment we measured shape and the moment we measured nectar) prevented us from detecting QTLs with the normal model. Categorizing individuals in "low producing" and "high producing" and using the binary QTLs detection model permitted to detect one QTL. We also tried to study sugar concentration in nectar (using a Hand Held Brix Refractometer 0-32°, Fisher) but faced the same variability problems and did not succeed in detecting any QTL (data not shown). The confidence region of the QTL for nectar volume was very large. Other QTLs could likely be detected with stricter growing conditions to decrease intra individual variations and a larger sample size. Indeed, similar studies generally detected several QTLs explaining nectar volume variation. Bradshaw et al. (1998) detected two QTLs for nectar volume explaining together 63.4% of total variance. Similarly, Stuurman et al. (2004) also detected two QTLs associated with nectar volume in *Petunia* pollination syndromes. In contrast, Wessinger et al. (2014) detected only one QTL for nectar volume variation.

Multiple QTLs for corolla shape

We measured floral shape in order to first understand the genetic bases of the component of corolla shape evolution associated with pollination syndrome transition and second to understand the genetic bases of the components of corolla shape that are representative of differences between both parents, but not necessarily important for pollination syndrome identity.

For the shape component defined by pollination mode differences, we detected three independent QTLs. While we expected to detect only few QTLs for this "trait", to our knowledge, no other studies analysed QTLs for pollination syndrome evolution with geometric morphometrics and PCA methods. However we can compare our results with studies analysing shape differences in divergent environments in other organisms. Franchini et al. (2014) used the same method to study how body shape evolution related to trophic ecology between two fish species. Although their analyses involved

several individuals of both parent species but not from different species, they also detected relatively few QTLs (4), each one explaining less than 8% of variance.

Regarding shape differences between parents that are not necessarily associated with pollination syndromes, we detected seven distinct QTLs. Removing those that co-localized with QTLs of syndromes associated shape differences, four QTLs remained. Conceivably, shape may have evolved dramatically at the initial pollination syndrome transition, followed by gradual, small changes along the evolutionary tree (the two species studied are not sister species). Such hypothesis could be tested with repeated QTLs studies and phylogenetic comparative methods.

These results tend to show that genetic bases of shape evolution are more complex than those of colour and nectar volume. Concordant with our results, other studies of floral morphology detected multiple QTLs with small to moderate effects explaining morphological changes linked to pollination syndrome evolution. For example, Hodges et al. (2002) detected multiple QTLs for spur length or flower orientation differences between two *Aquilegia* species. Wessinger et al. (2014) detected multiple QTLs between two *Penstemon* species associated with morphological differences (explaining between 7.3 and 24.3% of the shape variance). Galliot et al. (2006) detected six QTLs explaining several component of flower size in *Petunia* representing each 2.7 to 41.6% of the variance, as well as four QTLs for nectar volume (explaining 4.2 to 39.1% of the variance). The same was detected for five morphological traits in *Leptosiphon* (each one represented by two to seven QTLs explaining two to 28% of the variance) (Goodwillie, Ritland & Ritland, 2006).

RADIALIS and *CYCLOIDEA*, two genes involved in the determination of floral zygomorphy (Preston, Martinez & Hileman, 2011), represent good candidates for explaining floral shape variation. To test this hypothesis, we genotyped and included them in our linkage map. None of them appears to be directly linked to the morphological transition between *R. auriculatum* and *R. rupincola*. In contrast, *CYCLOIDEA* is situated within the confidence region of one QTL explaining corolla tube opening, but it does not correspond to the marker with the maximum LOD score (Fig. 6 and supplementary Fig. 2). This suggests that none of the candidate genes are directly involved in corolla shape evolution in our model, at least not for the major shape differences between the pollination syndromes. Nevertheless, critical changes could involve gene expression regulation that could be missed with the current approach. Indeed, gene expression has been shown to be important in differentiating the shape of

generalist from specialist, as it is the differential dorsoventral expression of CYCLOIDEA-like genes that confers particular corolla shape (Hileman & Cubas, 2009).

Pollination syndrome evolution in the genus is summarized by morphological transition between *R. auriculatum* and *R. rupincola:*

Our results showed that generalist and hummingbird specialist species can be differentiated with only one shape component in *Rhytidophyllum* and *Gesneria*, which concurs with a broader study of the group (Joly et al. in prep). This shape component correlates with corolla tube opening in our hybrid population and discriminate the columnar shape of hummingbird pollinated species from the cup shape of generalists (Marten-Rodriguez, 2009). The strong correlation between the shape components obtained with the PCA at the genera level, among the parents and on the F2 hybrid population shows that the shape variation in the hybrid population correspond to flower shape variation observed at the level of genera. This suggests that morphological transition between *R. auriculatum* and *R. rupincola* is representative of the major morphological disparity between pollination syndromes at the genus level. To compare the genetic bases of simple traits and global shape, we measured both univariate traits and multivariate traits using geometric morphometrics. From the results obtained with these different methods, we reach two conclusions: (i) univariate morphological traits were strongly correlated with shape components suggesting that the information contained in simple traits is generally contained in geometric morphometrics data, and the latter contain more information than simple traits, and (ii) because one QTL was detected only when using univariate measure (QTL on LG16 for corolla tube opening), this suggests that due to their complexity, geometric morphometric traits may not catch exactly the same variation as linear traits or that relatively small segregating population size prevented from detecting QTL in different phenotypic measurement conditions. Such conclusions are somewhat different from those of Franchini et al. (2014) who detected different QTLs for geometric morphometric and simple traits measurements with only one co-localizing QTL explaining both global shape and an univariate trait. This reflects that different results might be expected in different systems and highlights the complementarity of both kinds of measures when analysing genetic architecture of shape evolution, particularly when using small population sizes.

Unlinked genetic variation and pollination syndrome transitions

Some authors argue that genetic correlation between traits could slow down adaptation (reviewed in Hendry 2013) and for this reason, we looked for genetic correlations between traits in our study. Morphological traits were found to be totally independent from colour and nectar characteristics. Wessinger et al. (2014) also found no correlation between shape components, flower colour or nectar volume, although they found weak but significant correlations between nectar concentration and some morphological traits. Galliot et al. (2006) in their segregating population detected a correlation between nectar volume and floral tube width. In their study of monkeyflowers, Bradshaw et al. (1998) detected epistatic interactions between the locus *YUP* involved in flower colour via carotenoid concentration and two other putative QTLs.

We found that QTLs for nectar, colour and shape are localized on different linkage groups or on different regions of the same group, making these traits genetically independent. Considering that the traits constituting pollination syndromes in the genus *Rhytidophyllum* are not strongly genetically linked (at least for the major components that we could detect in this study), we can consider that neither genetic constraints nor canalization played an important role in the pollination syndrome transition between *R. rupincola* and *R. auriculatum*. This tends to show that selection pressure exerted by pollinators – that is extrinsic factors – played a greater role in pollination syndrome evolution than intrinsic factors. Indeed, selection could have been exerted independently on each trait, and no developmental mechanism seems to have forced concerted evolution of pollination syndrome traits.

However, we still wonder if the same sequence of trait evolution took place between replicated evolutions in the whole group? This question could be answered with replicated QTLs studies on independent transitions and with the help of phylogenetic comparative methods. Accordingly, we agree with Moyle & Payseur (2009) that propose to combine comparative methods with QTLs to better understand evolutionary patterns of reproductive isolation or evolution in a wide scale.

Conclusion:

The present study enabled to detect major QTLs underlying the three major traits composing divergent pollination syndromes between two *Rhytidophyllum* species. Even if potentially several minors QTLs remained undetected, few major and independent regions for pollination syndrome development were identified. This independence of segregating traits suggests that selection pressure exerted by different

pollinators, rather than developmental constraints, was quite strong to make the different traits converge on a pollination syndrome.

ACKNOWLEGMENTS

We thank Nathalie Isabel who helped us in designing the experiment and François Lambert for sharing *Gesneria* and *Rhytidophyllum* shape data. We are also thankful to Stéphane Muños for his help with linkage map building and to Nancy Robert and Janique Perrault for maintaining the living plant collections at the Montreal Botanical Garden. We are grateful to Sebastien Renaut for corrections and comments on the manuscript.

503

504 REFERENCES

505 Adams DC, Otárola-Castillo E. 2013. Geomorph: An r package for the collection and analysis of
506 geometric morphometric shape data. *Methods in Ecology and Evolution* 4:393–399.

507 Ashman T-L, Majetic CJ. 2006. Genetic constraints on floral evolution: a review and evaluation of
508 patterns. *Heredity* 96:343–352.

509 Broman KW, Wu H, Sen S, Churchill G a. 2003. R/qtl: QTL mapping in experimental crosses.
510 *Bioinformatics* 19:889–890.

511 Camacho C, Coulouris G, Avagyan V, Ma N, Papadopoulos J, Bealer K, Madden TL. 2009. BLAST+:
512 architecture and applications. *BMC bioinformatics* 10:421.

513 Catchen JM, Amores A, Hohenlohe P, Cresko W, Postlethwait JH. 2011. Stacks: building and
514 genotyping Loci de novo from short-read sequences. *G3 (Bethesda, Md.)* 1:171–82.

515 Clabaut C, Bunje PME, Salzburger W, Meyer A. 2007. Geometric morphometric analyses provide
516 evidence for the adaptive character of the Tanganyikan cichlid fish radiations. *Evolution;*
517 *international journal of organic evolution* 61:560–78.

518 Dray S, Dufour a. B. 2007. The ade4 Package: Implementing the Duality Diagram for Ecologists.
519 *Journal of Statistical Software* 22:1 – 20.

520 Elshire RJ, Glaubitz JC, Sun Q, Poland J a, Kawamoto K, Buckler ES, Mitchell SE. 2011. A robust,
521 simple genotyping-by-sequencing (GBS) approach for high diversity species. *PloS one* 6:e19379.

522 Fenster CB, Armbruster WS, Wilson P, Dudash MR, Thomson JD. 2004. Pollination Syndromes and
523 Floral Specialization. *Annual Review of Ecology, Evolution, and Systematics* 35:375–403.

524 Franchini P, Fruciano C, Spreitzer ML, Jones JC, Elmer KR, Henning F, Meyer A. 2014. Genomic
525 architecture of ecologically divergent body shape in a pair of sympatric crater lake cichlid fishes.
526 *Molecular ecology* 23:1828–45.

527 Friedman J, Barrett SCH. 2009. Wind of change: new insights on the ecology and evolution of
528 pollination and mating in wind-pollinated plants. *Annals of botany* 103:1515–27.

529 Galliot C, Hoballah ME, Kuhlemeier C, Stuurman J. 2006. Genetics of flower size and nectar volume
530 in Petunia pollination syndromes. *Planta* 225:203–12.

531 Galliot C, Stuurman J, Kuhlemeier C. 2006. The genetic dissection of floral pollination syndromes.
532 *Current opinion in plant biology* 9:78–82.

533 De Givry S, Bouchez M, Chabrier P, Milan D, Schiex T. 2005. CART HAGENE: Multipopulation
534 integrated genetic and radiation hybrid mapping. *Bioinformatics* 21:1703–1704.

535 Goodwillie C, Ritland C, Ritland K. 2006. The genetic basis of floral traits associated with mating
536 system evolution in Leptosiphon (Polemoniaceae): an analysis of quantitative trait loci. *Evolution;*
537 *international journal of organic evolution* 60:491–504.

538 Hendry a P. 2013. Key questions in the genetics and genomics of eco-evolutionary dynamics. *Heredity*
539 111:456–66.

540 Hermann K, Kuhlemeier C. 2011. The genetic architecture of natural variation in flower morphology.
541 *Current opinion in plant biology* 14:60–5.

542 Hileman LC, Cubas P. 2009. An expanded evolutionary role for flower symmetry genes. *Journal of*
543 *biology* 8:90.

544 Hodges S a, Whittall JB, Fulton M, Yang JY. 2002. Genetics of floral traits influencing reproductive
545 isolation between Aquilegia formosa and Aquilegia pubescens. *The American naturalist* 159
546 Suppl :S51–60.

547 Jourjon MF, Jasson S, Marcel J, Ngom B, Mangin B. 2005. MCQTL: Multi-allelic QTL mapping in
548 multi-cross design. *Bioinformatics* 21:128–130.

549 Kakioka R, Kokita T, Kumada H, Watanabe K, Okuda N. 2013. A RAD-based linkage map and
550 comparative genomics in the gudgeons (genus Gnathopogon, Cyprinidae). *BMC genomics* 14:32.

551 Klingenberg CP, Leamy LJ, Routman EJ, Cheverud JM. 2001. Genetic architecture of mandible shape
552 in mice: effects of quantitative trait loci analyzed by geometric morphometrics. *Genetics* 157:785–
553 802.

554 Klingenberg CP. 2010. Evolution and development of shape: integrating quantitative approaches.
555 *Nature reviews. Genetics* 11:623–35.

556 Koressaar T, Remm M. 2007. Enhancements and modifications of primer design program Primer3.
557 *Bioinformatics* 23:1289–1291.

558 Langlade NB, Feng X, Dransfield T, Copsey L, Hanna AI, Thébaud C, Bangham A, Hudson A, Coen
559 E. 2005. Evolution through genetically controlled allometry space. *Proceedings of the National*
560 *Academy of Sciences of the United States of America* 102:10221–6.

561 Liu J, Shikano T, Leinonen T, Cano JM, Li M-H, Merilä J. 2014. Identification of major and minor
562 QTL for ecologically important morphological traits in three-spined sticklebacks (Gasterosteus
563 aculeatus). *G3 (Bethesda, Md.)* 4:595–604.

564 Martén-Rodríguez S, Fenster CB, Agnarsson I, Skog LE, Zimmer E a. 2010. Evolutionary breakdown
565 of pollination specialization in a Caribbean plant radiation. *The New phytologist* 188:403–17.

566 Martén-Rodríguez S, Almarales-Castro A, Fenster CB. 2009. Evaluation of pollination syndromes in
567 Antillean Gesneriaceae: evidence for bat, hummingbird and generalized flowers. *Journal of*
568 *Ecology* 97:348–359.

569 Martén-Rodríguez S, Fenster CB. 2008. Pollination ecology and breeding systems of five Gesneria
570 species from Puerto Rico. *Annals of botany* 102:23–30.

571 Moyle LC, Payseur B a. 2009. Reproductive isolation grows on trees. *Trends in ecology & evolution*
572 24:591–8.

573 Nakazato T, Rieseberg LH, Wood TE. 2013. The genetic basis of speciation in the Giliopsis lineage of
574 Ipomopsis (Polemoniaceae). *Heredity* 111:227–37.

575 Van der Niet T, Johnson SD. 2012. Phylogenetic evidence for pollinator-driven diversification of
576 angiosperms. *Trends in ecology & evolution* 27:353–61.

577 Orr HA. 2005. The genetic theory of adaptation: a brief history. *Nature reviews. Genetics* 6:119–27.

578 Perret M, Chautems A, Spichiger R, Barraclough TG, Savolainen V. 2007. The geographical pattern of
579 speciation and floral diversification in the neotropics: The tribe Sinningieae (Gesneriaceae) as a
580 case study. *Evolution* 61:1641–1660.

581 Preston JC, Martinez CC, Hileman LC. 2011. Gradual disintegration of the floral symmetry gene
582 network is implicated in the evolution of a wind-pollination syndrome. *Proceedings of the*
583 *National Academy of Sciences of the United States of America* 108:2343–8.

584 Quattrocchio F, Wing J, Woude K Van Der, Souer E, Vetten N De, Mol J, Koes R. 1998. Molecular
585 Analysis of the anthocyanin2 Gene of Petunia and Its Role in the Evolution of Flower Color.
586 :1433–1444.

587 Rogers SM, Tamkee P, Summers B, Balabahadra S, Marks M, Kingsley DM, Schluter D. 2012.
588 Genetic signature of adaptive peak shift in threespine stickleback. *Evolution; international journal*
589 *of organic evolution* 66:2439–50.

590 Rosas-Guerrero V, Aguilar R, Martén-Rodríguez S, Ashworth L, Lopezaraiza-Mikel M, Bastida JM,
591 Quesada M. 2014. A quantitative review of pollination syndromes: do floral traits predict effective
592 pollinators? *Ecology letters* 17:388–400.

593 Skog LE. A Study of the Tribe Gesnerieae , with a Revision of Gesneria (Gesneriaceae :
594 Gesnerioideae).

595 Slotte T, Hazzouri KM, Stern D, Andolfatto P, Wright SI. 2012. Genetic architecture and adaptive
596 significance of the selfing syndrome in Capsella. *Evolution; international journal of organic*
597 *evolution* 66:1360–74.

598 Stuurman J, Hoballah ME, Broger L, Moore J, Basten C, Kuhlemeier C. 2004. Dissection of floral
599 pollination syndromes in Petunia. *Genetics* 168:1585–99.

600 Tripp E a, Manos PS. 2008. Is floral specialization an evolutionary dead-end? Pollination system
601 transitions in Ruellia (Acanthaceae). *Evolution; international journal of organic evolution*
602 62:1712–37.

603 Wessinger CA, Hileman LC, Rausher MD, B PTRS. Identification of major quantitative trait loci
604 underlying floral pollination syndrome divergence in Penstemon Identification of major
605 quantitative trait loci underlying floral pollination syndrome divergence in Penstemon.

606 Wilson P, Wolfe AD, Armbruster WS, Thomson JD. 2007. Constrained lability in floral evolution:
607 counting convergent origins of hummingbird pollination in Penstemon and Keckiella. *The New*
608 *phytologist* 176:883–90.

609 Yuan Y-W, Sagawa JM, Young RC, Christensen BJ, Bradshaw HD. 2013. Genetic dissection of a
610 major anthocyanin QTL contributing to pollinator-mediated reproductive isolation between sister
611 species of Mimulus. *Genetics* 194:255–63.

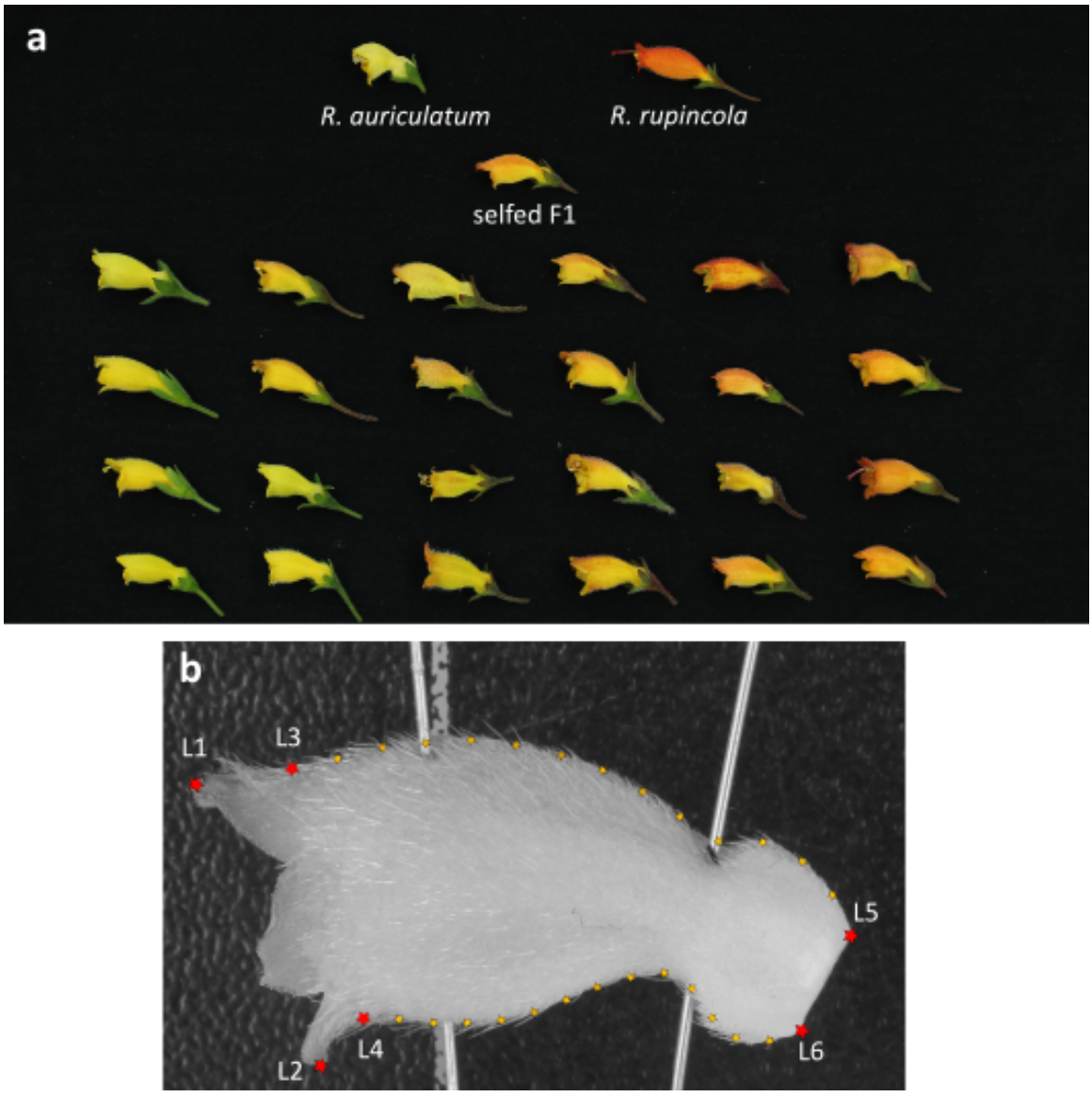

612

613

614 Figure 1: **Measure of shape variation in the hybrid population and parents**. (a) Flowers from both
615 parents (top row), the selfed F1 and samples from the F2 population; (b) position of landmarks on
616 corolla pictures- red stars represent landmarks and orange stars are semi-landmarks.

617

Figure 2 :

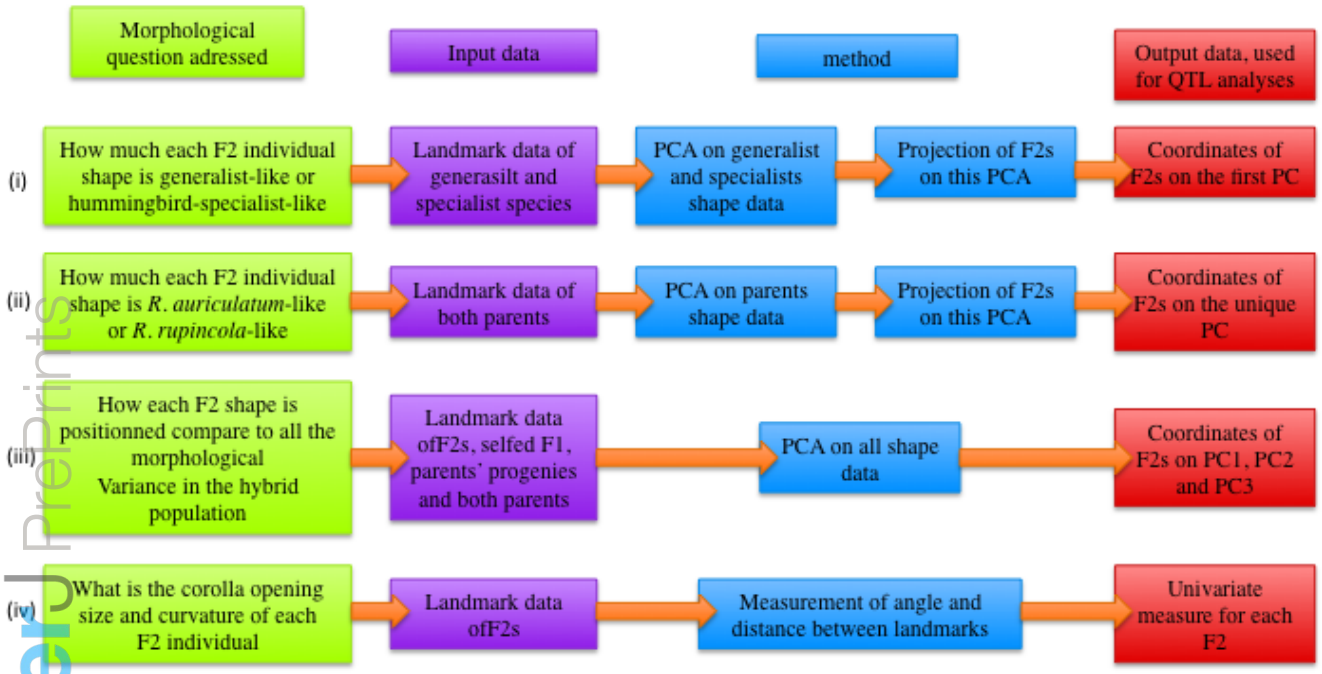

620 **Diagram presentation of the four morphological measurement approaches**. Numbers between
621 brackets refer to the methodology number in the main text.

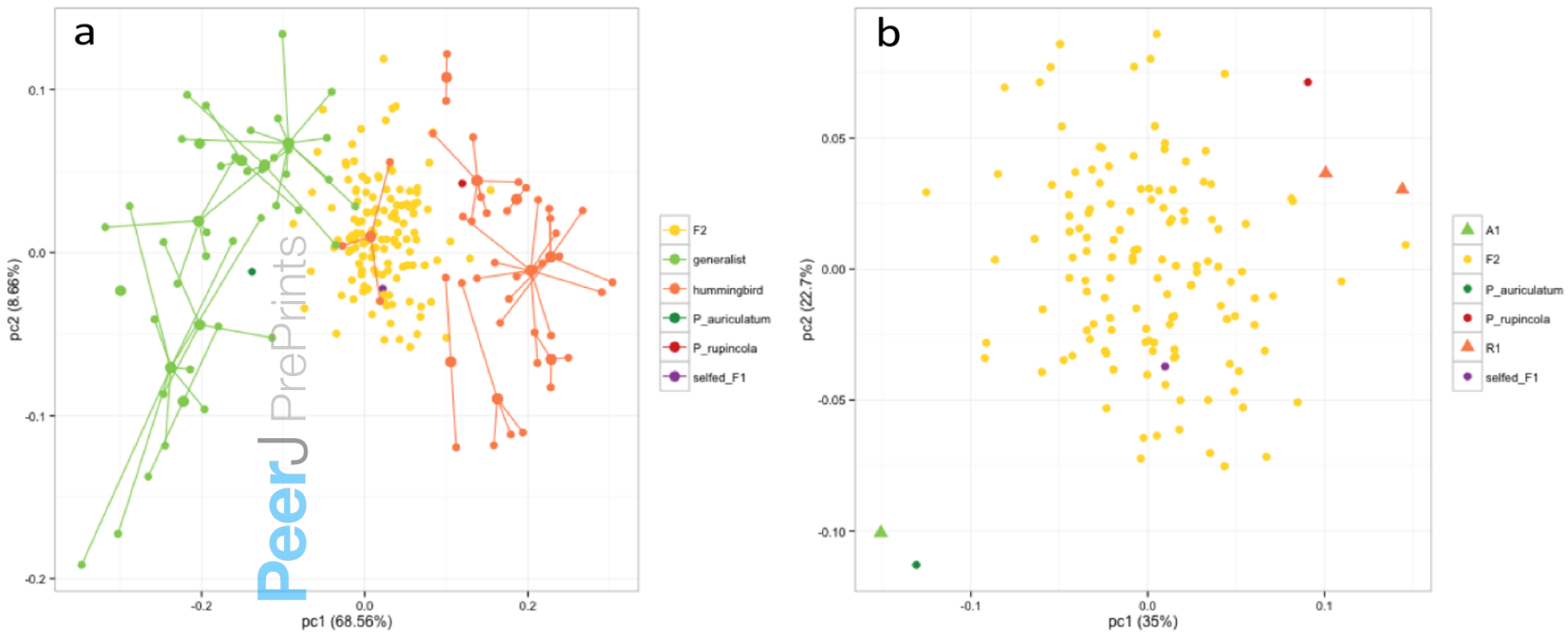

622

623

624 Figure 3: **Principal component analyses of shape**. (a) PCA performed on wild specimens from species with different pollination
625 syndromes and projection of the hybrid population on it; numbers between brackets are percentage of shape variance represented by each
626 axis. Large and small dots represent species mean shapes and individual shapes, respectively, and individuals that belong to a given species
627 are linked to it with a line. (b) PCA performed on the hybrid population where triangles represent parents' progeny.

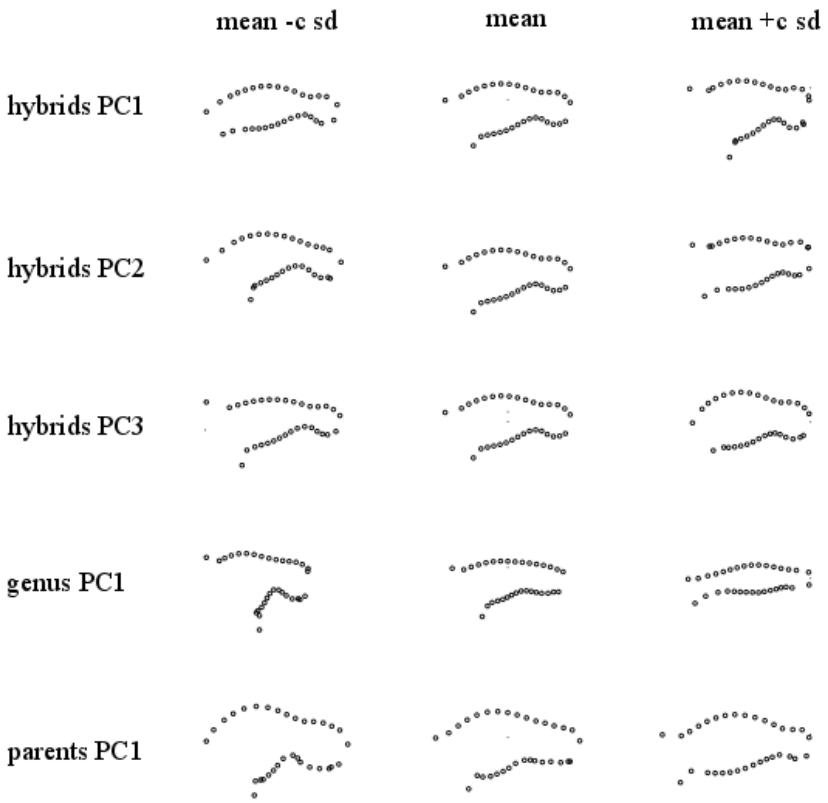

628

629 Figure 4 : **Shape variation associated with each principal component**. Sd : standard deviation, c = 1
630 for hybrids PCA, 0.5 for genus PCA and 0.2 for parents PCA.

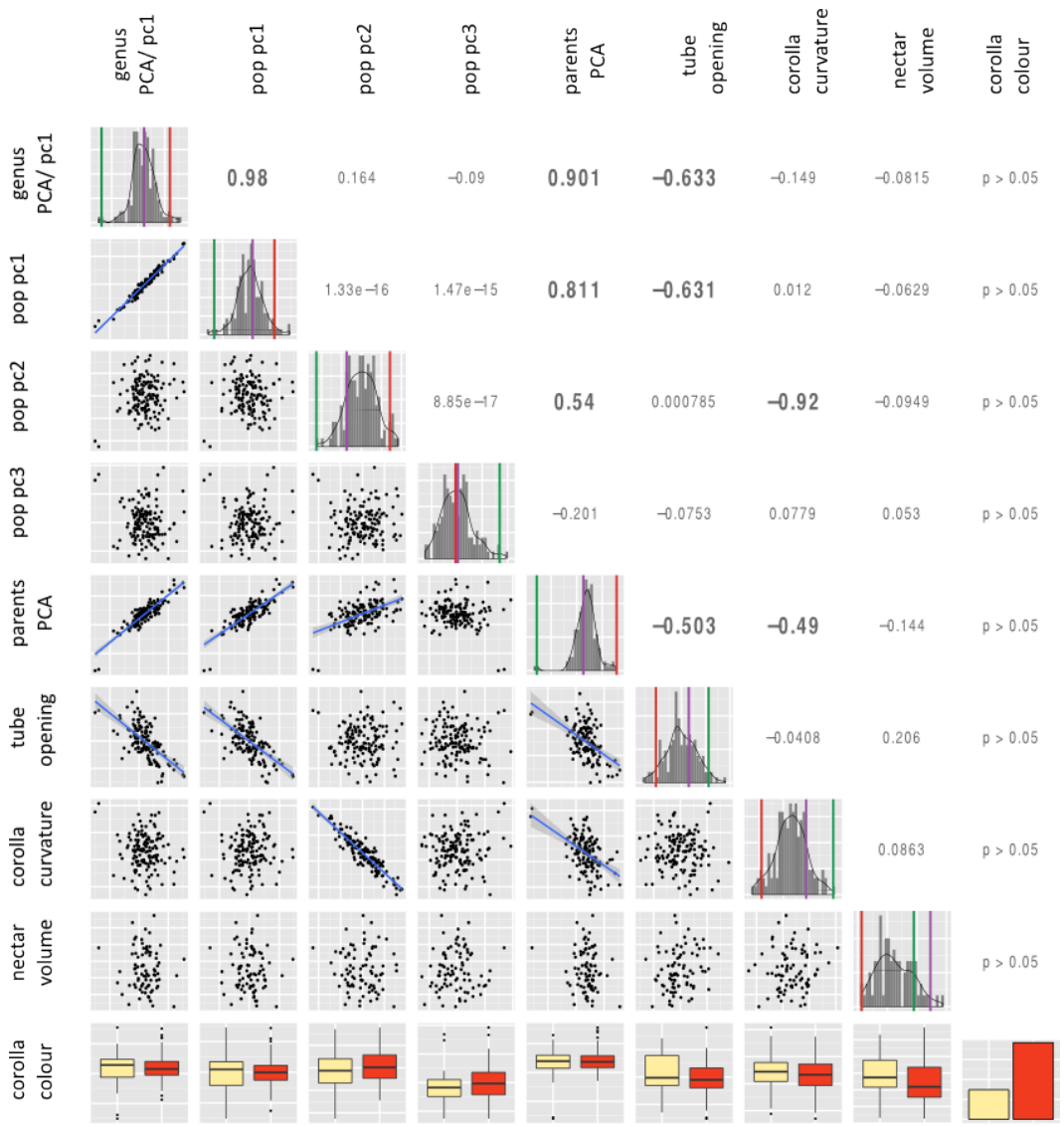

631

632 Figure 5: **Distribution and correlation among traits in the hybrid population**. Diagonal: traits
633 distribution, the vertical lines correspond to the value of parent *R. rupincola* (red), parent *R.*
634 *auriculatum* (green) and the selfed F1 (purple). Lower triangle: correlation among traits, if covariation
635 is significant after Sidak correction, the regression line was plotted. Upper triangle: regression
636 coefficient, in bold if correlation is significant.

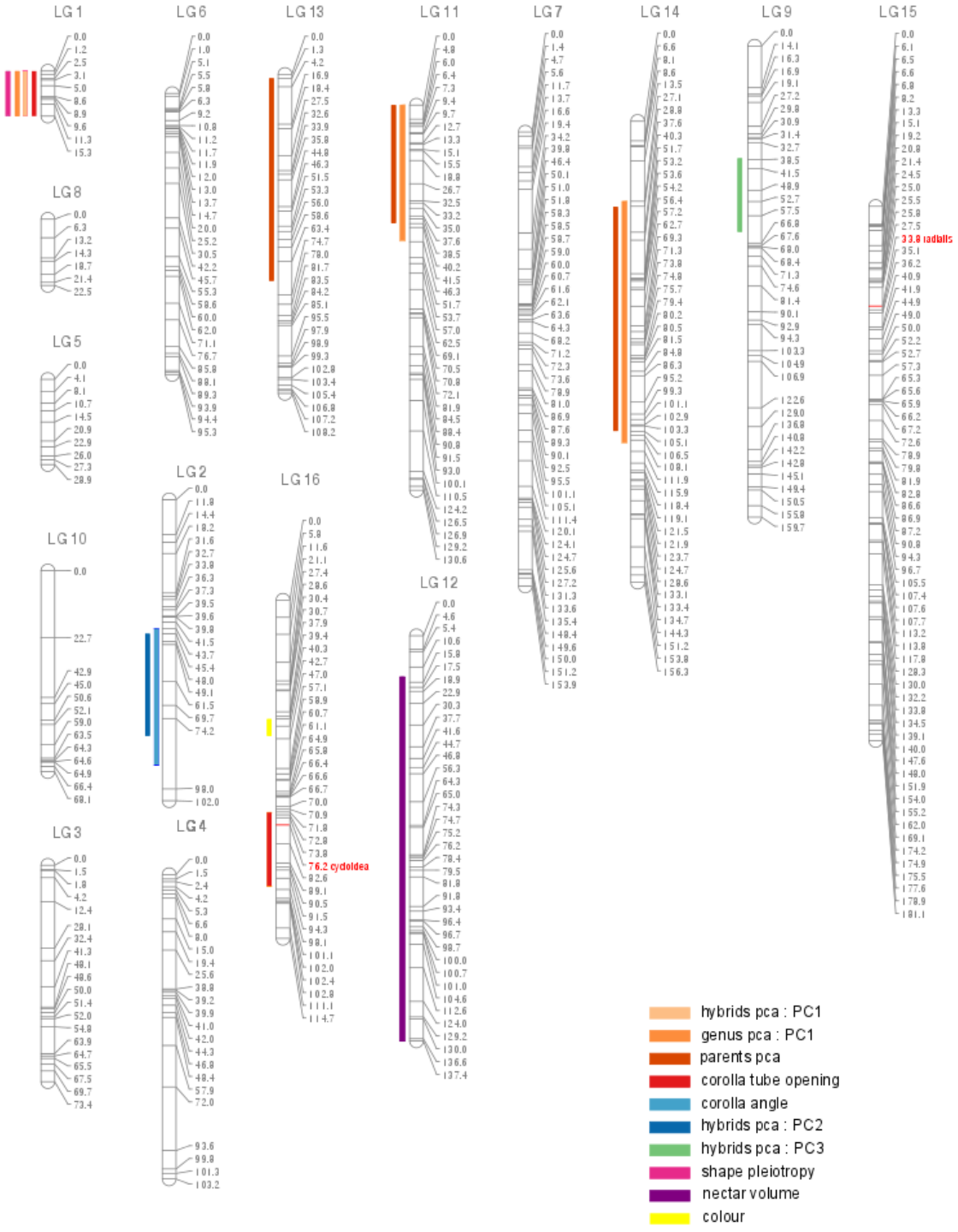

637

638 Figure 6: **Linkage map and position of QTLs**. QTLs positions are marked with 2-LOD confidence
639 region, numbers right to the linkage groups represent markers position in cM.

640

641 **Table 1: Information about linkage groups**

642

linkage group	nb. markers	Size (cM)	average distance between markers (cM)
LG1	12	15.3	1.7
LG2	23	102	4.86
LG3	22	73.4	3.86
LG4	26	103.2	4.49
LG5	11	28.9	3.21
LG6	36	95.3	3.07
LG7	59	153.9	3.02
LG8	7	22.5	3.75
LG9	46	159.7	4.2
LG10	13	68.1	5.68
LG11	48	130.6	3.19
LG12	40	137.4	3.71
LG13	34	108.2	3.49
LG14	57	156.3	3.13
LG15	81	181.1	2.62
LG16	44	114.7	2.94
total	559	1650.6	3.39

643

644

645 **Table 2: Position and effects of QTLs.** Positions are given in cM from the beginning of the linkage
646 group; confidence regions are calculated with 2 LOD score decrease.

trait		linkage group	position	confidence region	% variance explained	additive effect	t value
colour		LG16	43	40.3-46	-	-	-
nectar volume		LG12	41.6	14-137.4	-	-	-
PCA on hybrid population	pc1	LG1	11.3	0-15.3	15.13005	0.022562	4.487
	pc2	LG2	57	45.4-80	14.05676	0.019414	4.120
	pc3	LG9	19	38.63	14.89674	-0.016804	-4.705
	pleiotropy	LG1	0	0-15	-	-	-
PCA on parents	pc1	LG11	28	0-40	10.264	1.651e-02	4.209
		LG13	18	1.3-70	6.678	1.328e-02	3.493
		LG14	91	29-105	12.880	1.496e-02	4.347
PCA on genus	pc1	LG1	11.3	0-15.3	12.763	0.019736	4.698
		LG11	29	0-46	13.599	0.023374	4.938
		LG14	86.3	27.1-109	8.848	0.015323	3.625
corolla curvature		LG2	54	43.7-90	12.84071	-5.987	-3.684
corolla tube openning		LG1	15.3	0-15.3	12.48	-0.061357	-4.591
		LG16	85	72-97	12.36	-0.065712	-4.119

647

648